

JUNO and Neutrinoless Double Beta Decay

Shao-Feng Ge^{*1} and Werner Rodejohann^{†1}

¹Max-Planck-Institut für Kernphysik, Postfach 103980, 69029 Heidelberg, Germany

November 5, 2018

Abstract

We study the impact of the precision determination of oscillation parameters in the JUNO experiment on half-life predictions for neutrinoless double beta decay. We show that the solar neutrino mixing angle can be measured by JUNO with below 1% uncertainty. This implies in particular that the minimal value of the effective mass in the inverted mass ordering will be known essentially without uncertainty. We demonstrate that this reduces the range of half-life predictions in order to test this value by a factor of two. The remaining uncertainty is caused by nuclear matrix elements. This has important consequences for future double beta decay experiments that aim at ruling out the inverted mass ordering or the Majorana nature of neutrinos.

1. Introduction

With neutrino mass and lepton mixing firmly established as facts, a minimal basis to describe those phenomena has been developed. In this “3 Majorana neutrino paradigm”, three massive Majorana neutrinos are described by the neutrino mass matrix m_ν :

$$\mathcal{L} = \frac{1}{2} \nu_\alpha^T (m_\nu)_{\alpha\beta} \nu_\beta. \quad (1.1)$$

There are nine physical parameters in m_ν , usually parametrized as 3 masses, 3 mixing angles and 3 phases [1]. Within this simple framework, 3 tasks are eminent: determining the parameters as precisely as possible; checking if the minimal description (3 Majorana neutrino paradigm) is correct; explaining the measured parameter values.

Yet to be determined experimentally are the neutrino mass ordering, the octant of the atmospheric mixing angle, the Dirac CP phase, the absolute mass scale, whether neutrinos are Dirac or Majorana type fermions, and the Majorana CP phases if neutrinos are Majorana type. The first three play a role in neutrino oscillations, with which one can determine in total 6 parameters, 2 mass-squared differences, 3 angles and the Dirac phase. For the remaining parameters and properties non-oscillation experiments are inevitable. While our current information on the established oscillation parameters is already impressive [2], further improvement is of course needed. For instance, this is necessary to rule out flavor symmetry models (see e.g. [3]) or to check for new physics such as non-standard interactions, unitarity violation, long-range forces, etc. In this paper we address however another aspect of precision determination of neutrino oscillation parameters, namely its impact on neutrinoless double beta decay ($0\nu 2\beta$) [4, 5].

It is well-known that $0\nu 2\beta$ can in principle contribute to determining the Majorana or Dirac nature of neutrinos and also to the question of the neutrino mass ordering: in the standard paradigm the effective mass, on which the amplitude of the process depends, cannot vanish if the inverted mass ordering is realized. Therefore, if an oscillation experiment shows that neutrino masses have an inverted ordering, we know that the process must happen with a certain half-life $T_{1/2}^{\max}$. Not observing the decay with a half-life limit above $T_{1/2}^{\max}$ means that neutrinos are Dirac particles. In turn, not knowing the mass ordering and not observing the decay with a half-life limit above $T_{1/2}^{\max}$ rules out the inverted ordering in case neutrinos are Majorana particles¹. The timescales of determining the mass ordering [6] and reaching half-life limits in the inverted ordering regime are comparable [7] and subject to uncertainties, so both possibilities could happen. The effective mass value that future experiments need to reach in order to fulfill the two goals mentioned above needs to be known as precisely as possible, since it enters the half-life quadratically. If the experiment is dominated by background the situation is even worse.

^{*}gesf02@gmail.com

[†]werner.rodejohann@mpi-hd.mpg.de

¹Of course, new physics in neutrinoless double beta decay such as light sterile neutrinos or TeV-scale left-right symmetric models could modify such statements, see Refs. [4, 5] for a general discussion. We assume here that no contribution other than three massive Majorana neutrinos to double beta decay plays a role, thus we stay within the best motivated (standard) interpretation of the decay.

As argued in [8], the upper limit on the minimal half-life in the inverted ordering depends strongly on the solar neutrino mixing angle and its current uncertainty introduces a sizable uncertainty in half-life predictions. This “particle physics uncertainty” is of the same order as the “nuclear physics uncertainty”, i.e. the notorious nuclear matrix elements. Both uncertainties should be reduced. In this paper we demonstrate that future precision data on the oscillation parameters essentially removes the particle physics uncertainty. Towards this end, we apply the NuPro [9] package, written by one of us (SFG), to evaluate the precision with which the upcoming JUNO experiment [10] will determine the neutrino oscillation parameters and thus in particular the minimal effective mass in the inverted ordering. For demonstration, we will use JUNO as an example, we note that RENO-50 [11], with a very similar configuration, will reach similar precision.

We demonstrate that such medium baseline reactor experiments can measure the solar neutrino mixing angle with unprecedented precision of even less than 1%, in addition to their main goal of measuring the neutrino mass ordering. We translate this precision in half-life ranges of neutrinoless double beta decay for various isotopes and nuclear matrix element calculations. This will help $0\nu 2\beta$ experiments to possibly rule out the Majorana nature and evaluate their requirements to achieve this goal.

JUNO can not only determine the mass ordering, but also can measure the solar neutrino mixing angle with impressive precision at the same time. Thus, a single experiment can provide double beta decay experiments with all necessary information for ruling out the Majorana nature. To be more precise, the minimal value of the effective mass in the inverted mass ordering depends on the atmospheric mass-squared difference (very weakly on the solar one as well), θ_{12} and θ_{13} , i.e. the same set of parameters the electron neutrino survival probability in reactor experiments depends on. Thus, the latter have a direct correspondence to neutrinoless double beta decay experiments (and in principle also to single beta decay experiments).

Of course, if JUNO determines that neutrinos enjoy a normal mass ordering, the interesting link to double beta decay is somewhat lost, though the uncertainty of the effective mass in the normal ordering will still be reduced significantly. In case JUNO would not be able to determine the mass ordering because of limited energy resolution, we show that the precision on the solar neutrino mixing angle is not affected.

This paper is organized as follows. In Sec. 2 we discuss $0\nu 2\beta$ with three Majorana neutrinos and how the ability of ruling out the inverted ordering or the Majorana nature is related to the uncertainty of neutrino oscillation parameters. Then, we evaluate the precision that can be achieved at JUNO in Sec. 3, which is used in Sec. 4 to derive the required half-life sensitivity that $0\nu 2\beta$ experiments need to provide. Our conclusion can be found in Sec. 5.

2. Effective Neutrino Mass and Half-Life

Neutrinoless Double Beta Decay ($0\nu 2\beta$) is fundamentally important to particle physics as its observation implies lepton number violation, similar to the baryon number violation implied by an observation of proton decay. Several mechanisms for $0\nu 2\beta$ exist [4, 5]. In the best motivated interpretation, $0\nu 2\beta$ is mediated by Majorana neutrinos with mixing observed in neutrino oscillation experiments. The decay half-life can be expressed as

$$\left(T_{1/2}^{0\nu}\right)^{-1} = G^{0\nu} |M^{0\nu}|^2 \langle m_\nu \rangle^2, \quad (2.1)$$

where $G^{0\nu}$ is the well-known phase space factor and $M^{0\nu}$ the nuclear matrix element. Neutrino mass and mixing enters through the effective electron neutrino mass $\langle m_\nu \rangle$

$$\langle m_\nu \rangle = \left| c_s^2 c_r^2 m_1 + s_s^2 c_r^2 m_2 e^{i\alpha} + s_r^2 m_3 e^{i\beta} \right|, \quad (2.2)$$

with $(c_\alpha, s_\alpha) \equiv (\cos \theta_\alpha, \sin \theta_\alpha)$. Here, we have adopted the notation for mixing angles according to $\theta_a \equiv \theta_{23}$ denoting the atmospheric mixing angle, $\theta_r \equiv \theta_{13}$ the reactor mixing angle and $\theta_s \equiv \theta_{12}$ the solar mixing angle. For $0\nu 2\beta$, the only relevant mixing angles are θ_s and θ_r . Apart from these, the relevant parameters from the particle physics side involve the three neutrino mass eigenvalues m_i and the two Majorana CP phases α and β . Measured by neutrino oscillation experiments are the mixing angles and the two mass-squared differences, $\Delta m_s^2 \equiv m_2^2 - m_1^2$ and $\Delta m_a^2 \equiv |m_3^2 - m_1^2|$. Note that for the mass-squared difference between m_1^2 and m_3^2 only the magnitude has been measured. The different sign of Δm_a^2 leads to quite different mass patterns, the normal ordering (NO) with $m_1 < m_2 < m_3$ and the inverted ordering (IO) with $m_3 < m_1 < m_2$. Fig. 1 shows for both mass orderings the effective mass versus the smallest mass, as well as versus the neutrino mass parameters that are accessible in direct searches and cosmology. Both the current as well as future 3σ ranges, to be determined in the later part of the paper, are given.

Even with the absolute mass scale and mass ordering fixed, the effective electron neutrino mass $\langle m_\nu \rangle$ can still vary as a function of the two unknown Majorana CP phases α and β . For IO, the maximal and minimal values are

$$\langle m_\nu \rangle_{\max}^{\text{IO}} = \sqrt{m_3^2 + \Delta m_a^2 c_s^2 c_r^2} + \sqrt{m_3^2 + \Delta m_a^2 + \Delta m_s^2 s_s^2 c_r^2} + m_3 s_r^2, \quad (2.3a)$$

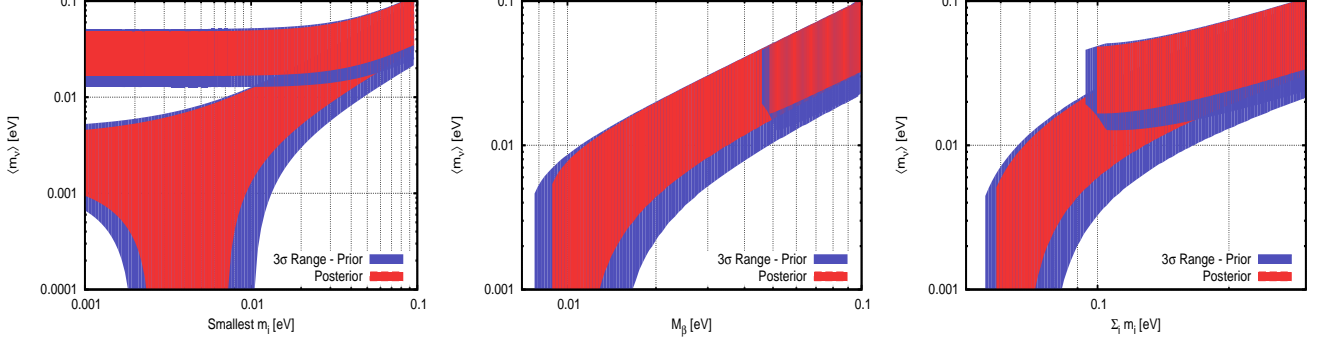


Fig. 1: The effective mass as a function of the smallest mass eigenvalue (m_1 for NO and m_3 for IO), β -decay mass $m_\beta = \sqrt{|U_{ei}|^2 m_i^2}$, and the sum of mass eigenvalues, within the 3σ range before (prior) and after (posterior) JUNO.

$$\langle m_\nu \rangle_{\min}^{\text{IO}} = \sqrt{m_3^2 + \Delta m_a^2 c_s^2 c_r^2} - \sqrt{m_3^2 + \Delta m_a^2 + \Delta m_s^2 s_s^2 c_r^2} - m_3 s_r^2. \quad (2.3b)$$

Since m_3 is the smallest mass, $s_r^2 \ll c_r^2$, $c_s^2 \simeq 2s_s^2$ and $\Delta m_a^2 \gg \Delta m_s^2$, the first term actually dominates over the second. As the two limits in (2.3) increase with m_3 , there is an universal lower limit [12] for IO when m_3 approaches zero (the lower limit $\langle m_\nu \rangle_{\min}^{\text{IO}}$ can also easily be extracted within a geometrical picture [13]):

$$\langle m_\nu \rangle_{\min}^{\text{IO}} \rightarrow \sqrt{\Delta m_a^2} (c_s^2 - s_s^2) c_r^2. \quad (2.4)$$

This value can put an upper bound on the half-life time $T_{1/2}^{0\nu}$ through (2.1). To exclude the inverted ordering, it is necessary for $0\nu 2\beta$ experiments to go beyond this limit. How precisely do we know this limit? Currently, the atmospheric mass-squared difference Δm_a^2 and the reactor mixing angle θ_r have been measured with precision at the few percent level. However, the solar mixing angle θ_s can contribute a significant uncertainty to $\langle m_\nu \rangle$ [8].

According to the latest global fit [2], the 3σ range of the solar mixing angle is $0.444 \leq \cos 2\theta_s \leq 0.250$. This implies at 3σ C.L. a total uncertainty of

$$\langle m_\nu \rangle_{\min}^{\text{IO}} = (0.0127 \dots 0.0198) \text{ eV}, \quad (2.5)$$

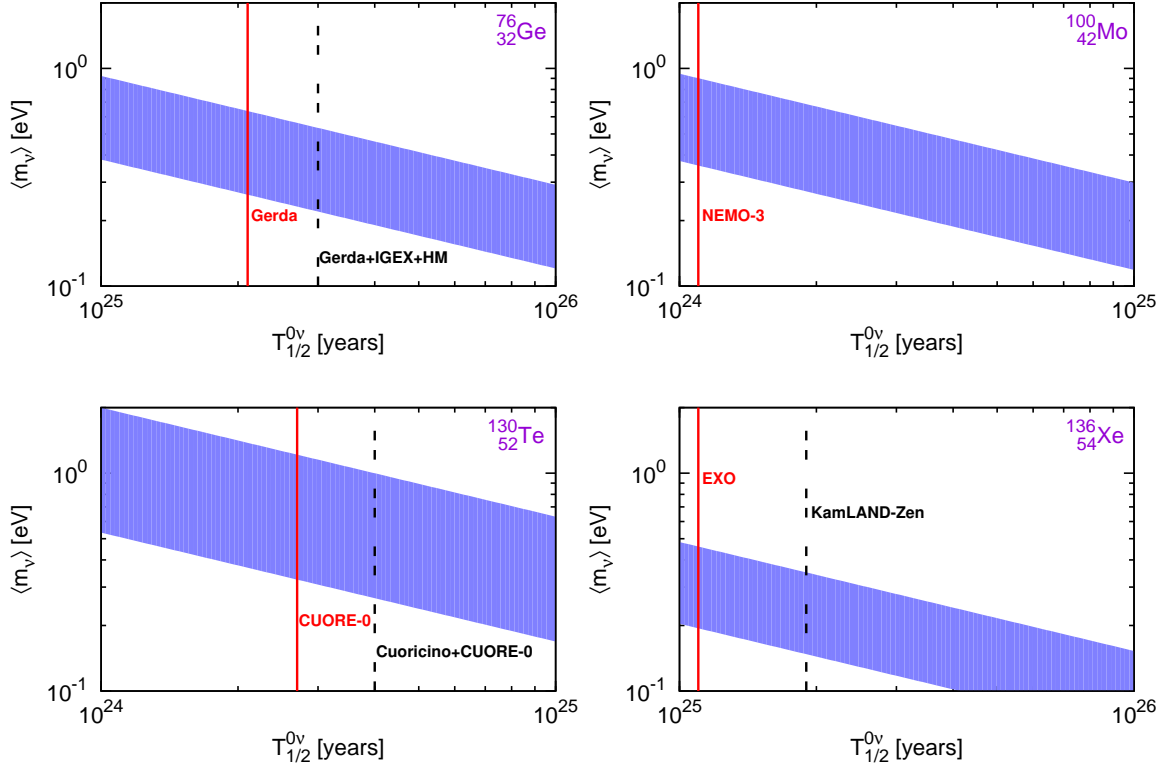


Fig. 2: Current limits on the effective mass (90% C.L.) for some isotopes for the range of nuclear matrix elements given in Table 1. The vertical lines are current experimental half-life limits.

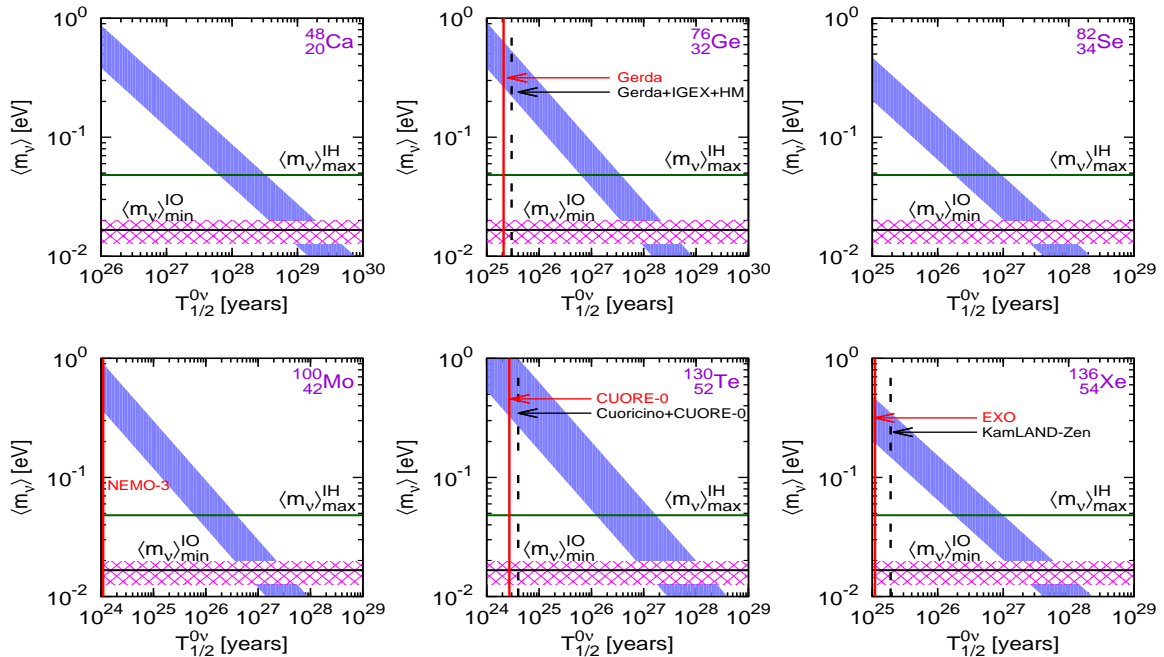


Fig. 3: Experimental constraints (90% C.L.) on the effective mass for some isotopes for the range of nuclear matrix elements given in Table 1. The vertical lines are current experimental half-life limits, the horizontal band is the current range for the minimal value in the inverted ordering, the lower solid line is after JUNO. The upper solid line is for the half-life to enter the inverted ordering regime, $\langle m_\nu \rangle^{\text{IH}}_{\text{max}} = \sqrt{\Delta m_a^2 c_r^2}$.

which varies by a factor of 1.6. Apart from $\langle m_\nu \rangle$, there is of course another source of uncertainty in predicting $T_{1/2}^{0\nu}$, namely the nuclear matrix elements $M^{0\nu}$. Their uncertainty, see Table 1, is of similar magnitude as the one coming from the oscillation parameters, in particular θ_s . Nuclear physics uncertainties will be addressed by the nuclear physics community. Here we focus on the particle physics uncertainty in $\langle m_\nu \rangle$, where progress is essentially guaranteed. In Fig. 2 we show, using the range of nuclear matrix elements from Table 1, for a subset of isotopes the current effective mass limits. The limits are

$$\begin{aligned}
 \langle m_\nu \rangle &\leq (0.22 \dots 0.53) \text{ eV} && \text{for } ^{76}\text{Ge}, \\
 \langle m_\nu \rangle &\leq (0.36 \dots 0.90) \text{ eV} && \text{for } ^{100}\text{Mo}, \\
 \langle m_\nu \rangle &\leq (0.27 \dots 1.00) \text{ eV} && \text{for } ^{130}\text{Te}, \\
 \langle m_\nu \rangle &\leq (0.15 \dots 0.35) \text{ eV} && \text{for } ^{136}\text{Xe},
 \end{aligned} \tag{2.6}$$

see also [14]. Note that these limits are not just for the three light neutrinos from Eq. (1.1), but include in principle possible sterile neutrinos up to masses slightly below the Fermi scale, i.e. the constraint is actually on $\sum_{1,n} U_{ei}^2 m_i$,

where the sum goes over all neutrinos below $m_n \simeq 50$ MeV. Note finally that the matrix elements depend roughly quadratically on the axial coupling constant g_A , and thus the effective mass limits in Eq. (2.6) would weaken by $(1.27/g_A)^2$ in case g_A would quench, i.e. become smaller as the nuclear mass becomes larger [15], see also [16]. The half-life limits we obtain in what follows would become stronger by a factor $(1.27/g_A)^4$. Fig. 3 shows for a larger subset of isotopes the effective mass limits as a function of half-life limits, showing in particular the necessary half-lives to rule out the inverted ordering, to be derived in Sec. 4. We also give the necessary half-lives to enter the regime in which for the inverted ordering in case of vanishing smallest mass the effective mass should lie, $\langle m_\nu \rangle^{\text{IH}}_{\text{max}} = \sqrt{\Delta m_a^2 c_r^2}$.

Note that the effective mass enters the half-life quadratically. If a $0\nu 2\beta$ experiment is dominated by background, the half-life that an experiment can reach is proportional to [17]

$$T_{1/2}^{0\nu} \propto a \times \epsilon \times \sqrt{\frac{M \times t}{B \times \Delta E}}, \tag{2.7}$$

where a is the isotopic abundance of the double beta emitter, M the fiducial mass, t the measuring time, ϵ the detection efficiency, ΔE the energy resolution around the peak, and B the constant background rate in units of counts/keV/kg/yr. We see that a factor of 2 uncertainty in the effective mass implies experimentally either a factor 4 in half-life or a combined factor of 16 in the experimental parameters in the square root in (2.7). For the current 3σ range, a variation by a factor of 1.6 in $\langle m_\nu \rangle^{\text{IO}}_{\text{min}}$ corresponds to a factor of 2.56 variation in the half-life, and thus a factor of 6 in the experimental parameters. Obviously this is challenging, especially when it comes to estimating the necessary size of the detector and the runtime to reach the limit of excluding IO.

In the next Section we will demonstrate how the precision on the effective mass can be improved at JUNO.

3. Precision Measurement of Solar Mixing Angle at JUNO

Reactor neutrinos are generated by nuclear reactions. Hence, their typical energy is in the MeV range which is not enough to produce muon or tau leptons in the final state. The only accessible oscillation channel is the electron survival probability P_{ee} , which depends on only two mixing angles, θ_r and θ_s , as well as two mass-squared differences:

$$P_{ee} = 1 - 4c_r^4 c_s^2 s_s^2 \sin^2 \Delta_{21} - 4c_s^2 c_r^2 s_r^2 \sin^2 \Delta_{31} - 4s_s^2 c_r^2 s_r^2 \sin^2 \Delta_{32}, \quad (3.1)$$

where $\Delta_{ij} \equiv (m_i^2 - m_j^2)L/4E_\nu$. Note that, just as for the effective mass, the atmospheric mixing angle θ_a and the Dirac CP phase δ_D are not involved. At short-baseline reactor experiments the dominant oscillation comes from the last two terms which are modulated by the large mass-squared difference $\Delta m_{32}^2 \approx \Delta m_{31}^2 = \Delta m_a^2$. The amplitude $\sim c_r^2 s_r^2$ is essentially independent of the solar mixing angle θ_s , hence short-baseline experiments can be used to measure the reactor mixing angle θ_r precisely. This has been and will be done by Daya-Bay, Double Chooz and RENO.

On the other hand, at longer baseline the contribution from the second term in (3.1) becomes dominant. On top of this slow oscillation, many fast oscillations occur. Note that the last two terms in (3.1) are not exactly the same. The difference between Δ_{31} and Δ_{32} is roughly $\Delta m_s^2/\Delta m_a^2 \approx 3\%$. In other words, there are two fast oscillation modes with slight difference. This can be used to determine the neutrino mass ordering [18, 19]. Depending on the neutrino mass ordering one frequency is faster than the other. To make the picture clear, we can formulate the oscillation (3.1) in terms of Δm_s^2 and Δm_a^2 ,

$$P_{ee} = 1 - 4c_r^4 c_s^2 s_s^2 \sin^2 \Delta_{21} - 4c_r^2 s_r^2 \sin^2 |\Delta_{31}| - 4s_s^2 c_r^2 s_r^2 \sin^2 \Delta_{21} \cos(2|\Delta_{31}|) \pm 2s_s^2 c_r^2 s_s^2 \sin(2\Delta_{21}) \sin(2|\Delta_{31}|), \quad (3.2)$$

where \pm corresponds to NO (+) and IO (-) respectively [20]. The difference in oscillation probability is equivalent to a relative phase shift between the two fast frequencies. Since the relative phase difference is only about $\Delta m_s^2/\Delta m_a^2 \approx 3\%$, it is necessary for the energy resolution to be better than 3%. By measuring the relative phase shift between the two fast frequencies, the neutrino mass ordering can be determined [21, 22, 23]. This corresponds to measuring the atmospheric mass-squared difference Δm_a^2 with precision around $\Delta m_s^2/\Delta m_a^2 \approx 3\%$, so that the tiny difference between Δm_{31}^2 and Δm_{32}^2 can be seen. To illustrate the picture, we show the event rate in Fig. 4. In the current study we focus on the JUNO configuration [10] with a 20kt liquid scintillator detector 52 km away from two reactor complexes with 36 GW total thermal power. The effective runtime is roughly 4.9 years (normal run time of 6 years with 300 effective days per year) and a detector energy resolution $3\%/\sqrt{E}$ (MeV) as benchmark.

One side product from this medium baseline reactor neutrino experiment is that the low frequency oscillation due to the second term in (3.1), which is essentially modulated by $4c_s^2 s_s^2$, can be used to measure the solar mixing angle θ_s precisely [24, 20]. This constraint mainly comes from the total event rate as shown in Fig. 4. Consequently, it will not be affected much by energy resolution, in contrary to the determination of the neutrino mass ordering. A rough estimate gives 1×10^5 events to be observed, with a statistically fluctuation of 3×10^{-3} . The actual uncertainty should be even further suppressed since not only the total event rate is measured, but a whole spectrum across the whole energy range. The position of the main peak in Fig. 4 can be used to constrain the corresponding oscillation frequency Δm_s^2 . Neither of them is sensitive to the energy resolution that the detector can finally achieve. Therefore a precise measurement of the solar mixing angle θ_s and the solar oscillation frequency Δm_s^2 is guaranteed. In Fig. 4, we also show the dependence on the solar mixing angle by plotting the event rates with central value $\sin^2 \theta_s = 0.323$ and 1σ upper limit $\sin^2 \theta_s = 0.339$, respectively.

We note that there is a study showing that the 5 MeV reactor anomaly can introduce a small shift in the best-fit of θ_s [25]. This anomaly is a bump in the ratio of measured and observed neutrino fluxes around energies of 5 MeV, as observed at Daya Bay [26], Double CHOOZ [27], and RENO [28, 29]. For a measurement of θ_s the anomaly can change the total event rate which is mainly controlled by $4c_s^2 s_s^2$ as we explained above. Consequently, the best fit of θ_s can be shifted away from its true value, although its uncertainty would not be affected much. This difficulty could in principle be overcome by an extra near detector. By comparing the event rates measured at near and far detectors, we can extract the oscillation probability between the two detectors that is purely due to the conventional three-neutrino oscillation. In addition, fitting the data with a parametrizable flux depletion/excess, such as gaussian-like shape as implemented in [25], can also correct the best fit-value.

In Fig. 5 we show the prior (input) and posterior (output) distributions of the solar mixing angle at JUNO, simulated with NuPro [9]. In total, the whole range from 1.8 MeV to 8 MeV is divided into 400 bins equally. Since the event rate in each bin is more than 20 events, the statistical fluctuation can be approximated as gaussian distribution. The χ^2 -function is defined as

$$\chi^2 \equiv \sum_i \frac{(\bar{N}_i - f N_i)^2}{\bar{N}_i} + \left[\frac{\Delta m_s^2 - \overline{\Delta m_s^2}}{\delta(\Delta m_s^2)} \right]^2 + \left[\frac{\Delta m_a^2 - \overline{\Delta m_a^2}}{\delta(\Delta m_a^2)} \right]^2 + \left[\frac{\sin^2 2\theta_r - \overline{\sin^2 2\theta_r}}{\delta(\sin^2 2\theta_r)} \right]^2 + \left[\frac{\sin^2 \theta_s - \overline{\sin^2 \theta_s}}{\delta(\sin^2 \theta_s)} \right]^2 + \frac{(f-1)^2}{0.01^2}, \quad (3.3)$$

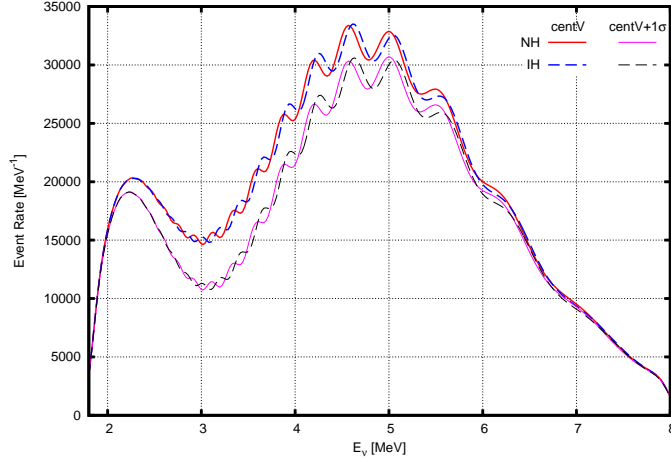


Fig. 4: The event rate of reactor neutrinos to be observed at JUNO. Two values of the solar neutrino mixing angle were used, $\sin^2 \theta_s = 0.323$ (thick lines) and $\sin^2 \theta_s = 0.339$ (thin lines).

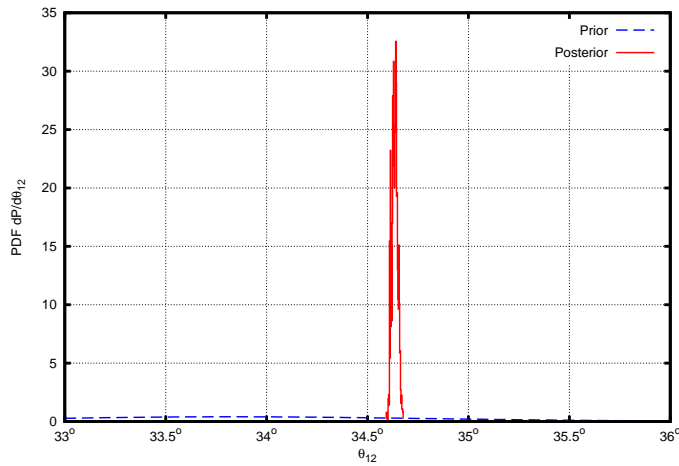


Fig. 5: Prior (input) and posterior (output) distributions of the solar mixing angle θ_s at JUNO.

with input values,

$$\Delta m_s^2 = (7.6 \pm 0.2) \times 10^{-5} \text{ eV}^2, \quad \Delta m_a^2 = (2.4 \pm 0.1) \times 10^{-3} \text{ eV}^2, \quad (3.4a)$$

$$\sin^2 2\theta_r = 0.089 \pm 0.005, \quad \sin^2 \theta_s = 0.323 \pm 0.016, \quad (3.4b)$$

according to the latest global fit [2] and Daya Bay measurement on θ_r [30]. In addition, the flux has an overall 1% uncertainty parametrized as an overall normalization f . Instead of minimization, the χ^2 -function (3.3) is used to sample the oscillation parameters, two mass-squared differences Δm_s^2 and Δm_a^2 as well as the two mixing angles θ_r and θ_s , with the Bayesian Nested Sampling algorithm [31]. Since there is no measurement of the two Majorana CP phases, they are randomly sampled between 0 and 2π . The sampled points are then analyzed to get the best fit values, uncertainties, and ranges of various functions of oscillation parameters simultaneously. In this way, the maginalization is carried out automatically.

It turns out that JUNO can significantly improve the uncertainty on θ_s from $\Delta[\sin^2 \theta_s] = 0.016$ down to 2.4×10^{-3} which is consistent with the rough estimation based on total event numbers. Correspondingly, the uncertainty $\Delta(\theta_s)$ is as small as 0.15° , roughly 4×10^{-3} of θ_s itself. At this precision, we can claim that the solar mixing angle θ_s as well as $\cos 2\theta_s$ are precisely known. In addition, the atmospheric mass-squared difference Δm_a^2 is measured with precision $\Delta[\Delta m_a^2]/\Delta m_a^2 \simeq 6 \times 10^{-3}$. In other words, there is almost no contribution from the neutrino mixing sector to the global lower limit of $\langle m_\nu \rangle_{\min}^{\text{IO}}$ as defined in (2.4). This will be quantified in the next Section.

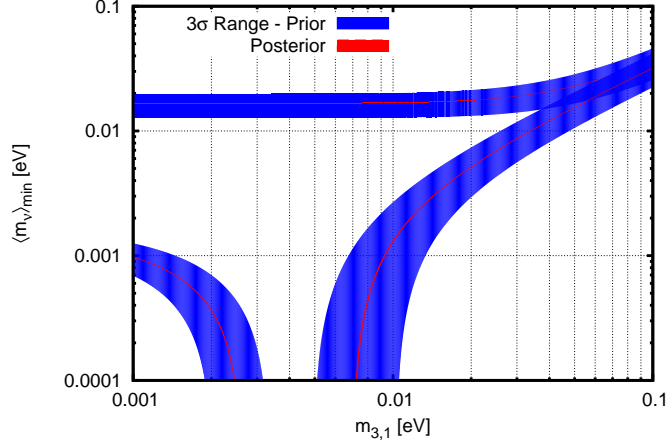


Fig. 6: The 3σ range of $\langle m_\nu \rangle_{\min}$ as a function of the lightest neutrino mass, m_1 for NO and m_3 for IO. All oscillation parameters, including the solar and reactor mixing angles, θ_s and θ_r , as well as the atmospheric and solar mass-squared differences, Δm_a^2 and Δm_s^2 , are varied in their corresponding 3σ ranges.

4. Implications for Double Beta Decay

With the solar mixing angle θ_s and the atmospheric mass-squared difference Δm_a^2 precisely measured by huge statistics and excellent energy resolution, respectively, the global lower limit on the effective electron neutrino mass (2.4) is actually fixed. In Fig. 6, we show the predicted $\langle m_\nu \rangle_{\min}^{\text{IO}}$ as a function of the smallest neutrino mass eigenvalue, in this case m_3 , with all other parameters, including the solar and reactor mixing angles, θ_s and θ_r , as well as the atmospheric and solar mass-squared differences, Δm_a^2 and Δm_s^2 , varied in their corresponding present and future 3σ ranges². At any value of m_3 , the uncertainty of the lower limit $\langle m_\nu \rangle_{\min}^{\text{IO}}$ is compressed to negligible size. Without JUNO, the value of $\langle m_\nu \rangle_{\min}^{\text{IO}}$ is unknown within a factor of roughly 1.6 at 3σ confidence level. After JUNO is included, it drops to the level of 2×10^{-3} , which is a huge improvement. It is safe to claim that $\langle m_\nu \rangle_{\min}^{\text{IO}}$ can be predicted almost precisely. For NO, the improvement is also significant, as depicted in Fig. 6. We also show in Fig. 1 the effective mass versus the smallest mass eigenvalue, as well as versus the neutrino mass parameters that are accessible in direct searches and cosmology, for both mass orderings. The improvement from the current 3σ ranges is obvious.

Fig. 7 shows the necessary half-lives to rule out the inverted ordering for the isotopes ^{48}Ca , ^{76}Ge , ^{82}Se , ^{100}Mo , ^{116}Cd , ^{130}Te , ^{136}Xe and ^{150}Nd . We have used a compilation of nuclear matrix elements which is summarized in Table 1. Also in this plot the improvement from the current range to the future situation is obvious. The shorter error bar corresponds to future uncertainty, which solely comes from the nuclear matrix elements. For instance, the range to go below $\langle m \rangle_{\min}^{\text{IO}}$ for ^{76}Ge is currently $T_{1/2}^{0\nu} = (3.7 \dots 52.3) \times 10^{27}$ yrs, while after JUNO it would be $T_{1/2}^{0\nu} = (5.3 \dots 31) \times 10^{27}$ yrs, the range is smaller by a factor 2.4. For ^{136}Xe the range is currently $T_{1/2}^{0\nu} = (1.1 \dots 14.3) \times 10^{27}$ yrs, which would improve to $T_{1/2}^{0\nu} = (1.5 \dots 8.4) \times 10^{27}$ yrs. See also Fig. 3 for the necessary half-lives to rule out (and reach, where the experimental improvement is of minor importance) the inverted ordering. For convenience, the ranges of half-lives have been summarized in Table 2.

5. Conclusion

The next generation of neutrino oscillation experiments will be able to provide mixing parameter determinations with remarkable precision. This has impact on a variety of aspects. Here we have studied inasmuch future reactor neutrino experiments can help in planing and interpreting future searches for neutrinoless double beta decay. The minimal value of the effective mass in the inverted ordering is currently uncertain by a factor of almost 2, comparable to the nuclear matrix element uncertainty. Facilities like JUNO can determine the minimal value of the effective mass with essentially no uncertainty, which fixes the half-life values corresponding to those extreme values, up to the nuclear matrix element uncertainties. The total uncertainty is therefore reduced by a factor 2, leaving further improvement to the nuclear physics community.

²For completeness, we also give in Fig. 6 the corresponding improvement for the minimal value in the normal ordering.

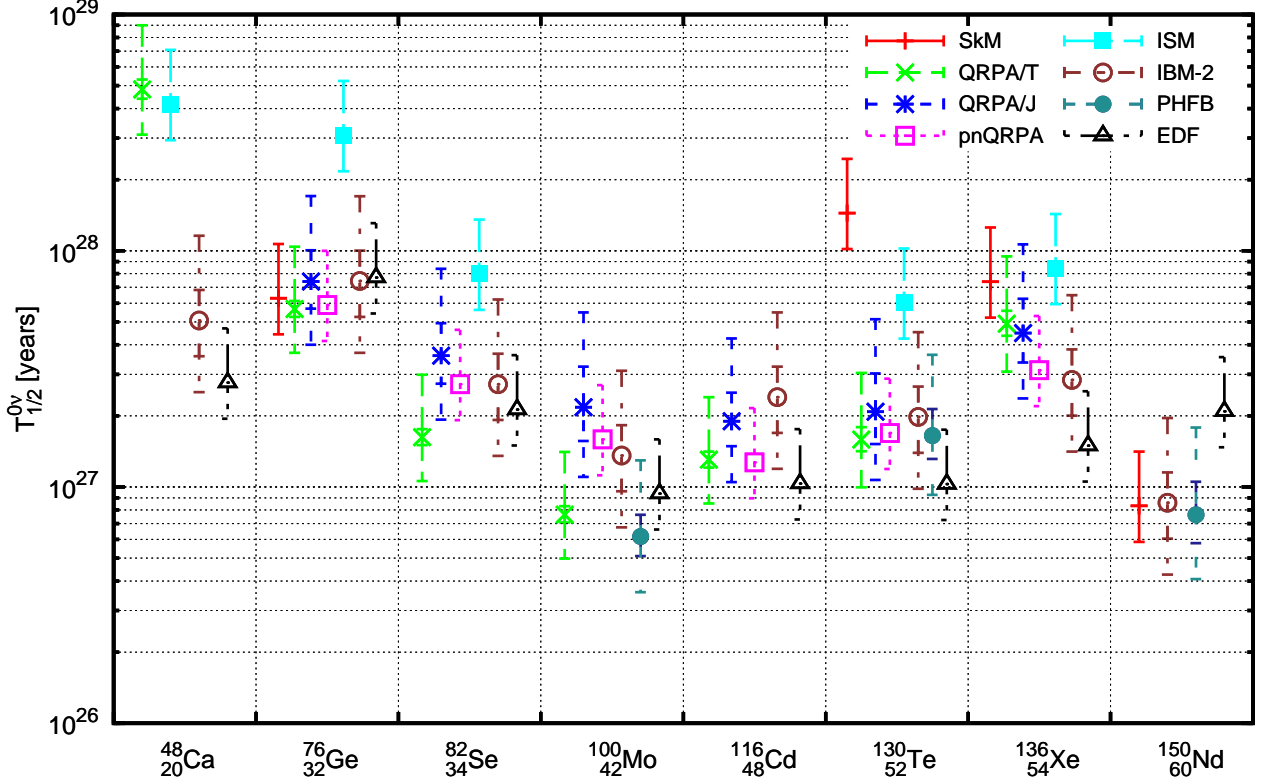


Fig. 7: The half-life $T_{1/2}^{0\nu}$ of neutrinoless double beta decay ($0\nu 2\beta$) to rule out the inverted ordering and its uncertainties. If one error bar is displayed, e.g. for SkM, the range is according to the current 3σ uncertainty in the oscillation parameters, which will be reduced to a single point after JUNO. If two error bars are displayed, e.g. for IBM-2, the nuclear matrix elements have a range, see Table 1. The larger error bar is then the combined uncertainty, from the matrix elements and the oscillation parameters in $\langle m \rangle_{\min}^{\text{IO}}$.

Acknowledgements

This work is partially supported by the Max Planck Society in the project MANITOP (WR).

References

- [1] K.A. Olive et al. *Review of Particle Physics*. *Chin.Phys.*, C38:090001, 2014.
- [2] D.V. Forero, M. Tortola, and J.W.F. Valle. *Neutrino oscillations refitted*. *Phys.Rev.*, D90(9):093006, 2014, [arXiv:1405.7540 [hep-ph]].
- [3] Andrew D. Hanlon, Shao-Feng Ge, and Wayne W. Repko. *Phenomenological consequences of residual \mathbb{Z}_2^s and $\overline{\mathbb{Z}}_2^s$ symmetries*. *Phys.Lett.*, B729:185–191, 2014, [arXiv:1308.6522 [hep-ph]].
- [4] Werner Rodejohann. *Neutrino-less Double Beta Decay and Particle Physics*. *Int.J.Mod.Phys.*, E20:1833–1930, 2011, [arXiv:1106.1334 [hep-ph]].
- [5] Heinrich Päs and Werner Rodejohann. *Neutrinoless Double Beta Decay*. 2015, [arXiv:1507.00170 [hep-ph]].
- [6] X. Qian and P. Vogel. *Neutrino Mass Hierarchy*. *Prog.Part.Nucl.Phys.*, 83:1–30, 2015, [arXiv:1505.01891 [hep-ex]].
- [7] Bernhard Schwingerheuer. *Status and prospects of searches for neutrinoless double beta decay*. *Annalen Phys.*, 525:269–280, 2013, 1210.7432.
- [8] Alexander Dueck, Werner Rodejohann, and Kai Zuber. *Neutrinoless Double Beta Decay, the Inverted Hierarchy and Precision Determination of θ_{12}* . *Phys.Rev.*, D83:113010, 2011, [arXiv:1103.4152 [hep-ph]].
- [9] Shao-Feng Ge. *NuPro: a simulation package of neutrino physics based on decomposition formalism in the propagation basis*. to appear.

- [10] Yu-Feng Li, Jun Cao, Yifang Wang, and Liang Zhan. *Unambiguous Determination of the Neutrino Mass Hierarchy Using Reactor Neutrinos*. *Phys.Rev.*, D88:013008, 2013, [arXiv:1303.6733 [hep-ex]].
- [11] Soo-Bong Kim. *New results from RENO and prospects with RENO-50*. 2014, [arXiv:1412.2199 [hep-ex]].
- [12] S. Pascoli and S. T. Petcov. *The SNO solar neutrino data, neutrinoless double beta decay and neutrino mass spectrum*. *Phys. Lett.*, B544:239–250, 2002, hep-ph/0205022.
- [13] Zhi-Zhong Xing and Ye-Ling Zhou. *Geometry of the effective Majorana neutrino mass in the $0\nu\beta\beta$ decay*. *Chin.Phys.*, C39(1):011001, 2015, [arXiv:1404.7001 [hep-ph]].
- [14] Pawel Guzowski, Luke Barnes, Justin Evans, Georgia Karagiorgi, Nathan McCabe, and Stefan Söldner-Rembold. *Combined limit on the neutrino mass from neutrinoless double- β decay and constraints on sterile Majorana neutrinos*. *Phys. Rev.*, D92(1):012002, 2015, 1504.03600.
- [15] J. Barea, J. Kotila, and F. Iachello. *Nuclear matrix elements for double- β decay*. *Phys.Rev.*, C87(1):014315, 2013, [arXiv:1301.4203 [nucl-th]].
- [16] Stefano Dell’Oro, Simone Marcocci, and Francesco Vissani. *New expectations and uncertainties on neutrinoless double beta decay*. *Phys. Rev.*, D90(3):033005, 2014, [arXiv:1404.2616 [hep-ph]].
- [17] F.T. Avignone, G.S. King, and Yu.G. Zdesenko. *Next generation double-beta decay experiments: Metrics for their evaluation*. *New J.Phys.*, 7:6, 2005.
- [18] S.T. Petcov and M. Piai. *The LMA MSW solution of the solar neutrino problem, inverted neutrino mass hierarchy and reactor neutrino experiments*. *Phys.Lett.*, B533:94–106, 2002, [arXiv:hep-ph/0112074].
- [19] Sandhya Choubey, S.T. Petcov, and M. Piai. *Precision neutrino oscillation physics with an intermediate baseline reactor neutrino experiment*. *Phys.Rev.*, D68:113006, 2003, [arXiv:hep-ph/0306017].
- [20] Shao-Feng Ge, Kaoru Hagiwara, Naotoshi Okamura, and Yoshitaro Takaesu. *Determination of mass hierarchy with medium baseline reactor neutrino experiments*. *JHEP*, 1305:131, 2013, [arXiv:1210.8141 [hep-ph]].
- [21] John Learned, Stephen T. Dye, Sandip Pakvasa, and Robert C. Svoboda. *Determination of neutrino mass hierarchy and θ_{13} with a remote detector of reactor antineutrinos*. *Phys.Rev.*, D78:071302, 2008, [arXiv:hep-ex/0612022].
- [22] Liang Zhan, Yifang Wang, Jun Cao, and Liangjian Wen. *Determination of the Neutrino Mass Hierarchy at an Intermediate Baseline*. *Phys.Rev.*, D78:111103, 2008, [arXiv:0807.3203 [hep-ex]].
- [23] Liang Zhan, Yifang Wang, Jun Cao, and Liangjian Wen. *Experimental Requirements to Determine the Neutrino Mass Hierarchy Using Reactor Neutrinos*. *Phys.Rev.*, D79:073007, 2009, [arXiv:0901.2976 [hep-ex]].
- [24] Mikhail Batygov, Stephen Dye, John Learned, Shigenobu Matsuno, Sandip Pakvasa, et al. *Prospects of neutrino oscillation measurements in the detection of reactor antineutrinos with a medium-baseline experiment*. 2008, [arXiv:0810.2580 [hep-ph]].
- [25] Emilio Ciuffoli, Jarah Evslin, Marco Grassi, and Xinmin Zhang. *Measuring θ_{12} Despite an Uncertain Reactor Neutrino Spectrum*. 2015, [arXiv:1503.05126 [hep-ph]].
- [26] Dmitry V. Naumov. *Recent results from Daya Bay experiment*. *EPJ Web Conf.*, 95:04043, 2015, [arXiv:1412.7806 [hep-ph]].
- [27] H. de Kerret. *Results from Double CHOOZ*. talk given on June 3, 2014 at *Neutrino 2014* in Boston.
- [28] S. B. Kim. *Observation of Reactor Antineutrino Disappearance at RENO*. talk given on June 4, 2012 at *Neutrino 2012* in Kyoto.
- [29] Seon-Hee Seo. *New Results from RENO and The 5 MeV Excess*. In *26th International Conference on Neutrino Physics and Astrophysics (Neutrino 2014) Boston, Massachusetts, United States, June 2-7, 2014*, 2014, [arXiv:1410.7987 [hep-ph]].
- [30] Dmitry V. Naumov. *Recent results from Daya Bay experiment*. *EPJ Web Conf.*, 95:04043, 2015, 1412.7806.
- [31] John Skilling. *Nested sampling for general Bayesian computation*. *Bayesian Analysis*, 1(4):833–859, 12 2006.
- [32] J. Barea, J. Kotila, and F. Iachello. *$0\nu\beta\beta$ and $2\nu\beta\beta$ nuclear matrix elements in the interacting boson model with isospin restoration*. *Phys.Rev.*, C91(3):034304, 2015, [arXiv:1506.08530 [nucl-th]].

- [33] M.T. Mustonen and J. Engel. *Large-scale calculations of the double- β decay of ^{76}Ge , ^{130}Te , ^{136}Xe , and ^{150}Nd in the deformed self-consistent Skyrme quasiparticle random-phase approximation.* *Phys.Rev.*, C87(6):064302, 2013, [arXiv:1301.6997 [nucl-th]].
- [34] Tomas R. Rodriguez and G. Martinez-Pinedo. *Energy density functional study of nuclear matrix elements for neutrinoless $\beta\beta$ decay.* *Phys. Rev. Lett.*, 105:252503, 2010, [arXiv:1008.5260 [nucl-th]].
- [35] P.K. Rath, R. Chandra, K. Chaturvedi, P. Lohani, P.K. Raina, et al. *Neutrinoless $\beta\beta$ decay transition matrix elements within mechanisms involving light Majorana neutrinos, classical Majorons, and sterile neutrinos.* *Phys.Rev.*, C88(6):064322, 2013, [arXiv:1308.0460 [nucl-th]].
- [36] J. Menendez, A. Poves, E. Caurier, and F. Nowacki. *Disassembling the Nuclear Matrix Elements of the Neutrinoless beta beta Decay.* *Nucl. Phys.*, A818:139–151, 2009, [arXiv:0801.3760 [nucl-th]].
- [37] Fedor Simkovic, Vadim Rodin, Amand Faessler, and Petr Vogel. *$0\nu\beta\beta$ and $2\nu\beta\beta$ nuclear matrix elements, quasiparticle random-phase approximation, and isospin symmetry restoration.* *Phys.Rev.*, C87(4):045501, 2013, [arXiv:1302.1509 [nucl-th]].
- [38] Osvaldo Civitarese and Jouni Suhonen. *Nuclear matrix elements for double beta decay in the QRPA approach: A critical review.* *J. Phys. Conf. Ser.*, 173:012012, 2009.
- [39] Juhani Hyvärinen and Jouni Suhonen. *Nuclear matrix elements for $0\nu\beta\beta$ decays with light or heavy Majorana-neutrino exchange.* *Phys. Rev.*, C91(2):024613, 2015.
- [40] J. Kotila and F. Iachello. *Phase space factors for double- β decay.* *Phys. Rev.*, C85:034316, 2012, [arXiv:1209.5722 [nucl-th]].

	SkM ^[33]	QRPA/T ^[37]	QRPA/J ^[38]	pnQRPA ^[39]	ISM ^[36]	IBM-2 ^[32]	PHFB ^[35]	EDF ^[34]	$G^{0\nu}$ ^[40]
$^{48}_{20}\text{Ca}$	–	0.541...0.594	–	–	0.61	$1.75 \times (1 \pm 0.16)$	–	2.37	23.29
$^{76}_{32}\text{Ge}$	5.09	5.157...5.571	4.029...5.355	5.26	2.30	$4.68 \times (1 \pm 0.16)$	–	4.60	2.218
$^{82}_{34}\text{Se}$	–	4.642...5.018	2.771...3.722	3.73	2.18	$3.73 \times (1 \pm 0.16)$	–	4.22	9.537
$^{100}_{42}\text{Mo}$	–	5.402...5.850	2.737...3.931	3.90	–	$4.22 \times (1 \pm 0.16)$	6.26 ± 0.63	5.08	14.94
$^{116}_{48}\text{Cd}$	–	4.040...4.367	3.034...3.935	4.26	–	$3.10 \times (1 \pm 0.16)$	–	4.72	15.68
$^{130}_{52}\text{Te}$	1.37	3.888...4.373	2.993...4.221	4.00	2.12	$3.70 \times (1 \pm 0.16)$	4.05 ± 0.49	5.13	13.35
$^{136}_{54}\text{Xe}$	1.89	2.177...2.460	2.053...2.802	2.91	1.77	$3.05 \times (1 \pm 0.16)$	–	4.20	13.69
$^{150}_{60}\text{Nd}$	2.71	–	–	–	–	$2.67 \times (1 \pm 0.16)$	2.83 ± 0.42	1.71	59.16

Table 1: Theoretical predictions for the nuclear matrix elements and the phase space factor in units of $10^{-26} \text{ yr}^{-1} \text{ eV}^{-2}$.

$T_{1/2}$ [yrs]	w/o JUNO	with JUNO	NME
	$\langle m_\nu \rangle_{\min}^{\text{IO}} = (0.0127 \dots 0.0198)$ eV	$\langle m_\nu \rangle_{\min}^{\text{IO}} = 0.0166$ eV	
^{48}Ca	$(1.95 \dots 4.69) \times 10^{27}$	2.76×10^{27}	$M_{\max}^{0\nu} = 2.37$
	$(3.74 \dots 9.01) \times 10^{28}$	5.30×10^{28}	$M_{\min}^{0\nu} = 0.55$
^{76}Ge	$(3.70 \dots 8.92) \times 10^{27}$	5.25×10^{27}	$M_{\max}^{0\nu} = 5.57$
	$(2.17 \dots 5.23) \times 10^{28}$	3.08×10^{28}	$M_{\min}^{0\nu} = 2.30$
^{82}Se	$(1.06 \dots 2.56) \times 10^{27}$	1.51×10^{27}	$M_{\max}^{0\nu} = 5.02$
	$(5.62 \dots 13.5) \times 10^{27}$	7.98×10^{27}	$M_{\min}^{0\nu} = 2.18$
^{100}Mo	$(3.59 \dots 8.65) \times 10^{26}$	5.10×10^{26}	$M_{\max}^{0\nu} = 6.89$
	$(2.28 \dots 5.48) \times 10^{27}$	3.23×10^{27}	$M_{\min}^{0\nu} = 2.74$
^{116}Cd	$(7.29 \dots 17.6) \times 10^{26}$	1.04×10^{27}	$M_{\max}^{0\nu} = 4.72$
	$(2.28 \dots 5.48) \times 10^{27}$	3.23×10^{27}	$M_{\min}^{0\nu} = 2.67$
^{130}Te	$(7.25 \dots 17.5) \times 10^{26}$	1.03×10^{27}	$M_{\max}^{0\nu} = 5.13$
	$(1.02 \dots 2.45) \times 10^{28}$	1.44×10^{28}	$M_{\min}^{0\nu} = 1.37$
^{136}Xe	$(1.06 \dots 2.54) \times 10^{27}$	1.50×10^{27}	$M_{\max}^{0\nu} = 4.20$
	$(5.94 \dots 14.3) \times 10^{27}$	8.43×10^{27}	$M_{\min}^{0\nu} = 1.77$
^{150}Nd	$(4.08 \dots 9.82) \times 10^{26}$	5.78×10^{26}	$M_{\max}^{0\nu} = 3.25$
	$(1.47 \dots 3.55) \times 10^{27}$	2.09×10^{27}	$M_{\min}^{0\nu} = 1.71$

Table 2: Half-life ranges to rule out the inverted ordering before (after) JUNO. For each isotope, the first row corresponds to the range (or value) for the largest matrix element $M_{\max}^{0\nu}$, while the second row is the range (value) for the smallest matrix element $M_{\min}^{0\nu}$. Before JUNO (w/o), $\langle m_\nu \rangle_{\min}^{\text{IO}}$ varies due to the particle physics uncertainty which essentially vanishes after JUNO.